Available online at www.sciencedirect.com
SCIENCE DIRECT®
Journal of Sound and Vibration 267 (2003) 591–604
JOURNAL OF SOUND AND VIBRATION
www.elsevier.com/locate/jsvi

A dynamic model for an asymmetrical vehicle/track system

K. Hou*, J. Kalousek, R. Dong[1]

Centre for Surface Transportation Technology, National Research Council, 3250 East Mall, Vancouver, BC, Canada

Accepted 9 May 2003

Abstract

A finite element model to simulate an asymmetrical vehicle/track dynamic system is proposed in this paper. This model consists of a 10-degree-of-freedom (d.o.f.) vehicle model, a track model with two rails, and an adaptive wheel/rail contact model. The surface defects of wheels and rails can be simulated with their geometry and an endless track model is adopted in the model. All time histories of forces, displacements, velocities and accelerations of all components of the vehicle and track can be obtained simultaneously. By using this model, one can study the effect that wheel/rail interaction from one side of the model has on the other. This can be done for many asymmetrical cases that are common in railway practice such as a wheel flat, wheel shelling, out-of-round wheel, fatigued rail, corrugated rail, head-crushed rail, rail joints, wheel/rail roughness, etc. Only two solutions are reported in this paper: steady state interaction and a wheel flat.

1. Introduction

Studies on railway dynamics have been performed for almost a century. Knothe and Grassie [1] have reviewed the historical background of modelling of railway vehicle/track interaction. Timoshenko [2] started to study vehicle/track dynamics to examine the effect of wheel flats in 1926. In the last century hundreds of papers and reports about the vehicle/track dynamics have been published.

The techniques to study vehicle/track interaction can be divided into two parts: frequency-domain modelling and time-domain modelling. The frequency-domain technique is a simplified solution to wheel/rail interaction. It establishes a relationship between receptance and external force at different frequencies using a mathematical transformation under set assumptions, thereby

*Corresponding author. Present address: 8211 Carmel Road, Richmond, BC, Canada V7C 3R2.
E-mail address: keping@telus.com (K. Hou).
[1] Present address: 23, Wood Crest Drive, Morgantown, WV 26505, USA.

0022-460X/$ - see front matter © 2003 Elsevier Ltd. All rights reserved.
doi:10.1016/S0022-460X(03)00726-0

avoiding the solution of complicated differential equations. Timoshenko [2] was the first person to use the frequency-domain technique to analyze track dynamics and he proposed the concept of receptance for a continuously supported Euler beam. The receptance of an Euler beam on a separate layer of rigid sleepers was first calculated by Sato [3]. Grassie et al. [4] have systematically introduced the technique and studied the dynamic response of railway track using a frequency-domain modelling technique. Thompson [5] also used the technique to implement a model of noise generation from a wheel/rail dynamic system.

Time-domain modelling is a technique used to solve the wheel/rail interaction in the time domain. Displacements, velocities, accelerations and forces on all components in the vehicle/track system can be solved in the time domain by coupling the track model, vehicle model and wheel/rail contact model. The vibration frequencies of the different components can be calculated using the displacement-time relationship. There are several notable researchers who have made contributions to time-domain modelling for the vehicle/track dynamic system, and who are developing vehicle/track time-domain models. The models developed before 1980 were simple due to the limitations of computer technology at that time. Cai and Raymond [6] have presented a wheel/rail and track dynamic model, considering a 4-d.o.f. vehicle model and 40-sleeper long discretely supported track model. Nielsen and Igeland [7,8] have developed a vehicle/track dynamic model, in which a finite element model of track containing 30 sleepers with fixed boundaries at both ends was used. Dong [9,10] successfully developed a finite element time-domain model for vehicle/track interaction. This model can provide responses for all components of vehicle and track as the vehicle moves along the track. Defects can be simulated on the wheels and the rails in the vehicle/track system. Zhai and Sun [11] have developed a model to simulate the vehicle/track dynamic system with a 10-d.o.f. vehicle model and a 3-layer track model.

However, all the vehicle/track models mentioned above are based on the assumption of vehicle/track symmetry in order to simplify the calculation. Generally, this simplification is reasonable for many cases, such as steady state situations; wheel flats, which always appear at the same position of both wheels on a wheelset; burned rail, which always forms at the same position on both rails; etc. However, in many cases defects of wheels and rails are not symmetric. For example, railhead crush always forms on one rail. This defect forms due to inclusions inside the rail, and it is very rare for inclusions to appear inside both rails at the same position. Corrugation is another asymmetrical example. Some corrugations take place only on one side of the track, other corrugations have a phase difference between the two rails even though they form on both rails. There are many other asymmetrical cases, such as geometric misalignment, rail joints, wheel shelling, fatigue damage on top of the rail, and so on. For the asymmetrical cases, unfortunately, the symmetric vehicle/track model is not accurate. Therefore, an asymmetrical vehicle/track model should be developed to solve asymmetrical problems.

An asymmetrical vehicle/track dynamic model, which is a finite element time-domain model, is presented in this paper. The model combines three models together: a 10-d.o.f. vehicle model, a two-layer track model with two rails and an adaptive wheel/rail contact model. The combined model can simulate a vehicle moving on track continuously for as long as needed. All time histories of forces, displacements, velocities and accelerations of the related components of the vehicle and the track can be solved simultaneously. The responses of all components of the vehicle and the track to any wheel/rail defects can be obtained with this program.

By using this computer model, two cases have been studied: the steady state situation and one leading wheel with a flat. The vehicle/track interactions on both sides of the track will be exhibited.

2. Model of vehicle/track dynamics

The vehicle/track dynamic model consists of three models: the 10-d.o.f. vehicle model, the track model with two rails and the adaptive wheel/rail contact model. A wheel flat geometry will also be introduced in this section.

2.1. Vehicle model

A two level suspension vehicle model is employed. The wheelset and the bogie are connected by the primary suspension while the car body is supported on the bogie through the secondary suspension. A more realistic vehicle model incorporating two wheelsets, two bogie sideframes, and half a car body is represented as a 10-d.o.f. model as shown in Fig 1. In this model, each wheelset has vertical and rotational d.o.f. at its centre (u_{W1}, u_{W2}, θ_{W1} and θ_{W2}). The bogies have vertical (u_{B1} and u_{B2}) and pitch (θ_{B1} and θ_{B2}) d.o.f. while the car body has vertical (u_C) and rotational (θ_C) d.o.f.

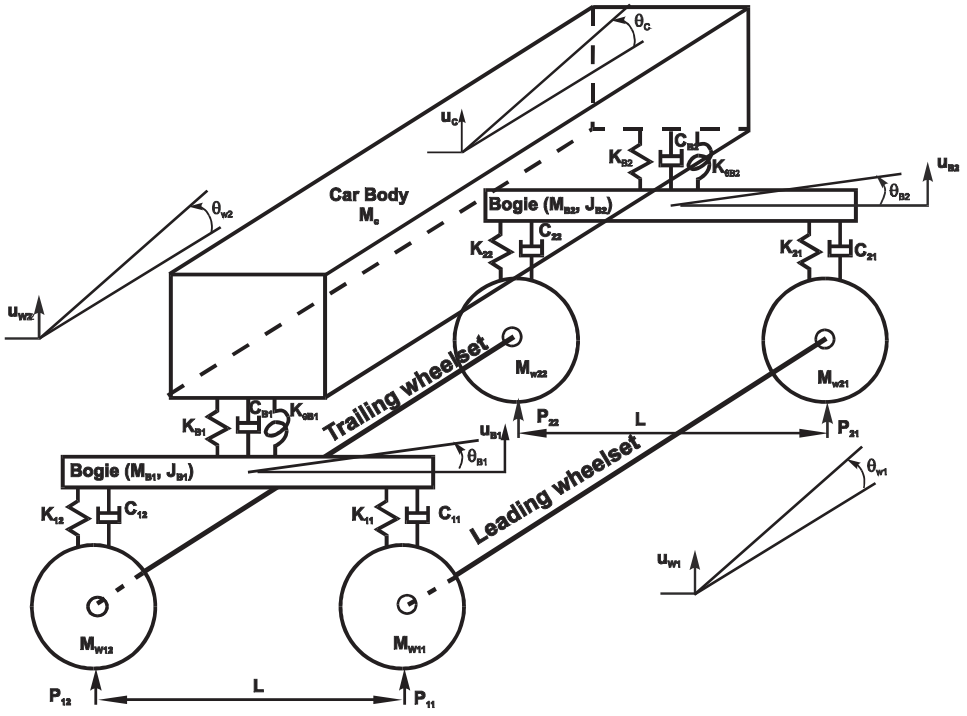

Fig. 1. Vehicle model.

The motion equation for the 10-d.o.f. model can be expressed as

$$[\mathbf{M}]\{\ddot{\mathbf{u}}\}+[\mathbf{C}]\{\dot{\mathbf{u}}\}+[\mathbf{K}]\{\mathbf{u}\}=\{\mathbf{F}\}, \tag{1}$$

where [**M**], [**C**] and [**K**] are matrices of mass, damping and stiffness, and the vectors of displacement {**u**} and force {**F**} are given by

$$\{\mathbf{u}\} = \{\, u_{W1} \quad \theta_{W1} \quad u_{W2} \quad \theta_{W2} \quad u_{B1} \quad \theta_{B1} \quad u_{B2} \quad \theta_{B2} \quad u_C \quad \theta_C \,\}^{\mathrm{T}},$$

$$\{\mathbf{F}\} = \{\, F_{W1} \quad M_{W1} \quad F_{W2} \quad M_{W2} \quad F_{B1} \quad M_{B1} \quad F_{B2} \quad M_{B2} \quad F_C \quad M_C \,\}^{\mathrm{T}}.$$

2.2. Track model

The track studied in this paper is a two-layer model consisting of sleepers, rail pads, ballast, subgrade and two rails, as shown in Fig. 2. The finite element method was used to analyze the track system. The differential equation of the track model has the same form as Eq. (1). However, the contents of the vectors and matrices of the track model are different from the vehicle model. The force and displacement vectors include all components of forces and displacements at all nodes on the track.

The track is divided into a number of units in the model. Each unit comprises one sleeper, seven ballast spring–dampers and two pieces of rail between two centres of adjacent sleeper spans. Each piece of rail consists of four elements in a track unit section.

The rails are simulated with Timoshenko beams that rest on discrete pad-sleeper-ballast supports. Each element of the rails (Fig. 3) is a two-node element with four degrees of freedom at each node. The nodal degrees of freedom of the element are described as a vector form

$$\{\boldsymbol{\eta}^e\} = \left\{ u_n^e, \Phi_n^e, \left(\frac{\partial u}{\partial x}\right)_n^e, \left(\frac{\partial \Phi}{\partial x}\right)_n^e, u_{n+1}^e, \Phi_{n+1}^e, \left(\frac{\partial u}{\partial x}\right)_{n+1}^e, \left(\frac{\partial \Phi}{\partial x}\right)_{n+1}^e \right\}^{\mathrm{T}}, \tag{2}$$

where u is the vertical displacement, Φ is the rotational angle, e is the element number and n and $n+1$ are the global node numbers at each side of the element. It is assumed that u and Φ are

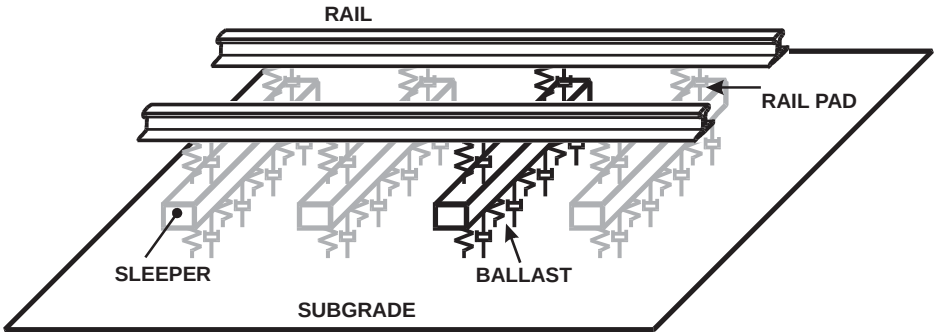

Fig. 2. Two layer track model.

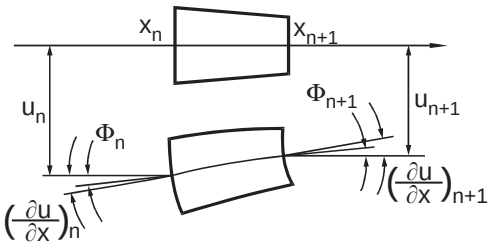

Fig. 3. Finite element Timoshenko beam model.

represented by the polynomial expressions of the form:

$$u = \sum_{i}^{8} \alpha_i \eta_i^e, \quad \Phi = \sum_{i}^{8} \beta_i \eta_i^e, \tag{3}$$

where $\alpha_i(\xi)$ and $\beta_i(\xi)$ are cubic polynomial shape functions:

$$\begin{aligned}
&\alpha_1 = \beta_2 = (2 - 3\xi + \xi^3)/4,\\
&\alpha_3 = \beta_4 = h(1 - \xi)(1 - \xi^2)/8,\\
&\alpha_5 = \beta_6 = (2 + 3\xi - \xi^3)/4,\\
&\alpha_7 = \beta_8 = -h(1 + \xi)(1 - \xi^2)/8,\\
&\alpha_2 = \alpha_4 = \alpha_6 = \alpha_8 = \beta_1 = \beta_3 = \beta_5 = \beta_7 = 0,
\end{aligned} \tag{4}$$

where h is the length of the beam element. By using the energy method, matrices of mass, stiffness and damping and a force vector for the each beam element can be expressed as follows.

The stiffness matrix is given by

$$\begin{aligned}
k_{ij} = &\frac{TGh}{2} \int_{-1}^{1} A_r \left(\frac{4}{h^2} \frac{\mathrm{d}\alpha_i}{\mathrm{d}\xi} \frac{\mathrm{d}\alpha_j}{\mathrm{d}\xi} \mathrm{d}\xi + \beta_i \beta_j - \frac{2}{h} \beta_i \frac{\mathrm{d}\alpha_j}{\mathrm{d}\xi} - \frac{2}{h} \beta_j \frac{\mathrm{d}\alpha_i}{\mathrm{d}\xi} \right) \mathrm{d}\xi\\
&+ \frac{2E}{h} \int_{-1}^{1} I_r \frac{\mathrm{d}\beta_i}{\mathrm{d}\xi} \frac{\mathrm{d}\beta_j}{\mathrm{d}\xi} \mathrm{d}\xi + \frac{h}{2} \int_{-1}^{1} k_f \alpha_i \alpha_j \, \mathrm{d}\xi, \quad i,j = 1,2,\ldots,8,
\end{aligned} \tag{5}$$

where k_{ij} is the component of stiffness matrix, A_r is the cross-section area of the rail, E and G are the elastic modulus and shear modulus, respectively, I_r is the rail second moment of area, T is the Timoshenko shear coefficient of the rail and k_f is the foundation stiffness of the beam.

The mass matrix is given by

$$m_{ij} = \frac{\rho h}{2} \int (A_r \alpha_i \alpha_j + I_r \beta_i \beta_j) \, \mathrm{d}\xi, \quad i,j = 1,2,\ldots,8, \tag{6}$$

where m_{ij} is the component of the mass matrix and ρ is the density of the rail material.

The damping matrix is

$$c_{ij} = \frac{h}{2} \int_{-1}^{1} c_r \alpha_i \alpha_j \, \mathrm{d}\xi, \quad i,j = 1,2,\ldots,8, \tag{7}$$

where c_{ij} is the component of the damping matrix and c_r is the foundation damping coefficient of the beam.

The force vector is

$$F_i = \frac{h}{2}\int_{-1}^{1} p(\xi, t)\alpha_i \, d\xi, \quad i = 1, 2, \ldots, 8, \tag{8}$$

where F_i is the force component of the force vector and p is the distributed force on rail.

The sleepers are simplified as Euler–Bernoulli beams. The sleeper is modelled as a beam with six elements (7 nodes) in the cross-track direction. There are two d.o.f. (vertical displacement and bending angle) at each node on the sleeper. It is defined that the sleeper can rotate as a rigid body in the plane of longitudinal and vertical directions. Therefore another d.o.f. of a sleeper, a rotation angle, is added at the two nodes on the sleeper just under the rails.

The rail pads are treated as distributed massless spring–dampers inserted between the rails and sleepers. Ballast is also considered as a set of massless spring–damper elements distributed between the sleepers and subgrade. The subgrade is assumed to form a rigid support. There are a total of 56 d.o.f. in one unit of the track.

The number of units for the entire FE track model is determined by considering the distance effect of the wheel/rail interaction. If, at a point far from the wheel/rail contact, the displacement of the track is insignificant, then that point is the boundary of the track model. Normally, a distance of eight sleepers beyond the two wheel/rail contact points under the leading and trailing wheels is a good base for this model. In this paper the total length of the track is 20 sleepers.

The unit matrices of mass, stiffness and damping are banded matrices with size 56×23, where 23 is the halfwidth of the matrix band. In order to solve the equations, global matrices of mass, stiffness and damping have to be established. If a 20-sleeper track is considered, 20 unit matrices should be installed into the global matrices. The size of the global matrices will be 968×23.

When the vehicle moves along the track, the contact positions are approaching the boundary of one end of the track. The effects of the vehicle forces can not be neglected at the approached boundary because the distance between the leading wheel and the boundary gets shorter and shorter. However, it is impossible for a model to have infinite track length. A cutting and merging method developed by Dong [9] is adapted in this study. This is accomplished by cutting a unit at the trailing end of the track and adding a new unit at the leading end of the track, after the vehicle has travelled a distance of one unit, as shown in Fig. 4. In this way, only the effective part of the

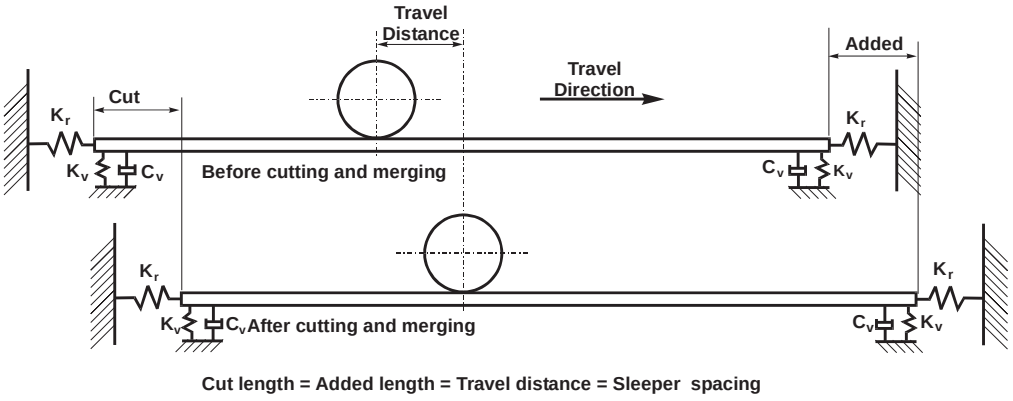

Fig. 4. The cutting and merging method for a track model.

track is kept in the model and the vehicle is able to travel on the track indefinitely. High frequency displacement fluctuations may be introduced in the cutting and merging process. These disturbances can be satisfactorily minimized when viscous damping is imposed at both rail ends.

2.3. Wheel/rail contact model

The adaptive wheel/rail contact model illustrated in Fig. 5 is used in this paper. The wheel/rail contact is represented by a set of uniformly distributed linear springs that have the same stiffness. This model is equivalent to the Hertzian contact theory. Using Hertzian contact theory, the elastic deformation of the wheel and rail can be calculated. The elastic deformation caused by real wheel/rail contact is assumed to be the same as the deformation caused by compression of a group of equidistantly distributed sub-springs under the same contact force. Since the contact force is known and the wheel/rail deformation is evaluated for the static case, the stiffness of the sub-springs can be obtained.

By solving the dynamic system, displacements of the wheel and rail can be obtained. An overlapped area between an undeformed wheel and rail is formed due to the displacements of the wheel and rail. It is assumed that the area is the total deformation of the wheel and rail, and also is a compression distribution of the sub-springs. Then a contact force between wheel and rail can be calculated by summing the forces on all sub-springs, which are the products of the compressed heights and stiffness of the sub-springs.

2.4. Defects

This vehicle/track model can simulate many wheel/rail defects such as wheel flats, wheel shelling, out-of-round wheels, rails with crushed head, fatigue damaged rails, rail joints, surface roughness, corrugated wheels and rails, etc. In these cases, train speed and axle load can vary over a wide range. Because four wheels and both sides of the track are considered, different wheel and rail profiles can be applied to the solution.

In this paper, only one defect case, the wheel flat, is investigated. The wheel flat can be represented as a circle with a chordal line, as shown in Fig. 6. The wheel profile can be

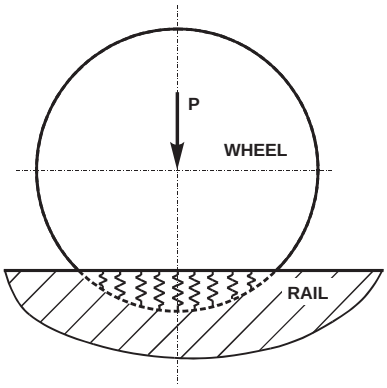

Fig. 5. Adaptive wheel/rail contact model.

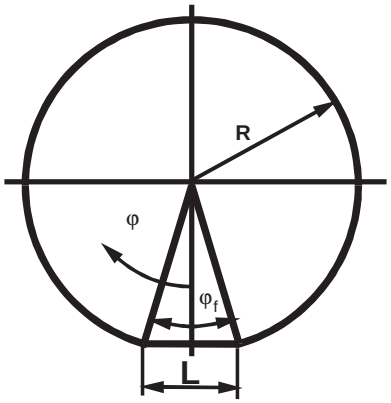

Fig. 6. Wheel flat model.

mathematically expressed as

$$r = \begin{cases} R, & |\varphi| \geqslant \varphi_f, \\ R\dfrac{\cos\varphi_f}{\cos\varphi}, & |\varphi| < \varphi_f, \end{cases} \tag{9}$$

where r is the distance from the wheel surface to the wheel centre, R is the wheel radius, φ is the angle co-ordinate, φ_f is half of the subtended angle of the flat and equal to $\sin^{-1}(L/2R)$ in which L is the circumferential length of the flat.

3. Computer program

The framework of the dynamic model is summarized in Fig. 7. The first task is to calculate the mass, stiffness and damping matrices for both the vehicle and the track after the individual parameters are read into the program. For cases with defects on the wheels or the rails or on both, the wheel and/or rail surface profiles should be entered in the program.

The time step of the program is chosen according to the speed. A reference time step (Δt_0) is 10^{-5} s for a speed of 54 km/h. The higher the vehicle speed is, the shorter the step is. A linear formula is used to select the time step:

$$\Delta t = \Delta t_0 \cdot V/54. \tag{10}$$

The reason to use such a short time step is to capture the high frequency dynamic responses from the vehicle/track system.

The wheels move along the rails step by step. In each step, the contact forces are calculated first based on the vertical displacements of the wheels and rails and surface profiles, and then the two dynamic systems of the vehicle and the track are solved separately. After that the calculation moves forward to another step. When the requirement for wheel travel distance is reached, the program stops.

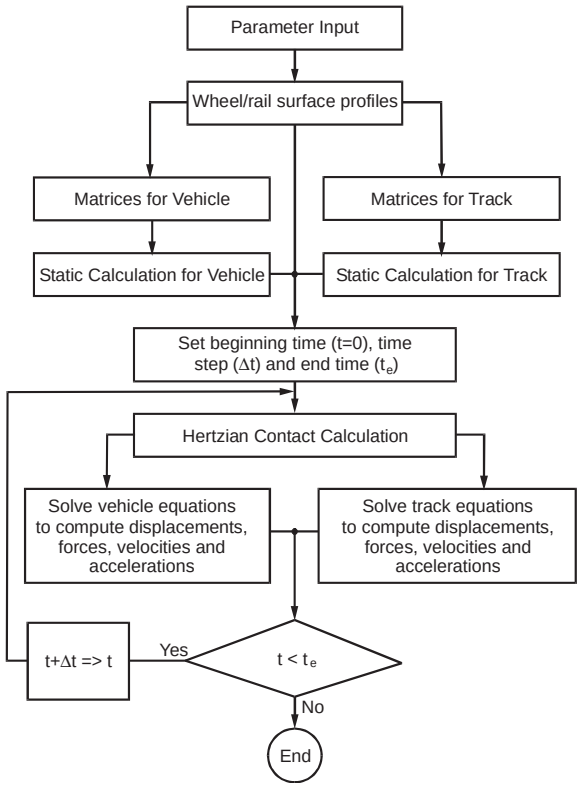

Fig. 7. Flow diagram of computer program.

4. Results and discussions

This asymmetrical vehicle/track model can be used to simulate many dynamic situations commonly seen in railway practice, such as steady state interaction, dynamic responses for wheel flat, wheel shelling, out-of-round wheels, top of rail fatigue, rail joints, wheel/rail corrugation, etc. Two cases, steady state interaction and a wheel flat on a leading wheel, are solved in this study to show the how the model works and what the model can do. The parameters used for the vehicle and track are given in Appendix A.

4.1. Steady state dynamic interaction

The so-called steady state interaction is a situation in which the rails are perfectly smooth, the wheels have no defects, the vehicle structure is symmetric, and the track structure is uniform. The study of steady state interaction provides information on the minimum dynamic force that would be generated as a vehicle runs on a track. Fig. 8 shows the displacements and dynamic forces of some components of the vehicle/track system in a steady state interaction when the vehicle travels on the track at a speed of 160 km/h.

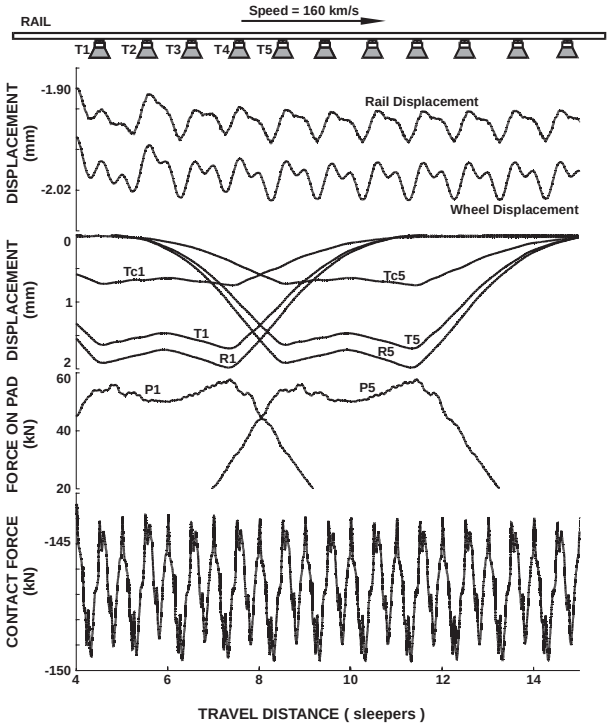

Fig. 8. Displacement of wheel, rail and sleepers, and wheel/rail contact force at the leading wheel contact point in the steady state interaction (T: sleeper, Tc: centre of sleeper, R: rail, P: pad).

The displacements of the wheel and the rail at the contact point are illustrated in Fig. 8. The two curves have the same trend with small differences. The differences cause the dynamic contact forces.

Fig. 8 also shows the displacement history of sleepers #1 and #5, the rail at the nodes supported by the sleepers and the centres of the sleepers when the vehicle is moving. There are two peaks on the curves because two wheelsets are taken into account. The leading wheel causes the first peak on the left side of the curves, and the trailing wheel causes the second peak on the right side of the curves. Fig. 8 shows that the deflections caused by the leading wheel are smaller than the deflections caused by the trailing wheel.

The forces on the pads are also plotted in Fig. 8. The force magnitude is about one third of the wheel/rail contact force in this case. The force history responds to the leading and trailing wheels as they pass over the sleepers.

Fig. 9 illustrates several samples of dynamic contact force at the wheel-rail interface in a steady state interaction at different speeds. In the majority of cases, the primary periodic wavelength in the time history of the dynamic force was equal to the sleeper spacing (0.6 m). This is obviously a result of the effect of the sleeper spacing. It is speculated that the spacing effect results primarily from the variation of overall track stiffness across each sleeper spacing. The wavelength, however, was surprisingly reduced to half of the sleeper spacing at 160 km/h (44 m/s). This interesting phenomenon may be explained from the analysis of the dynamic motions of the sleeper in the

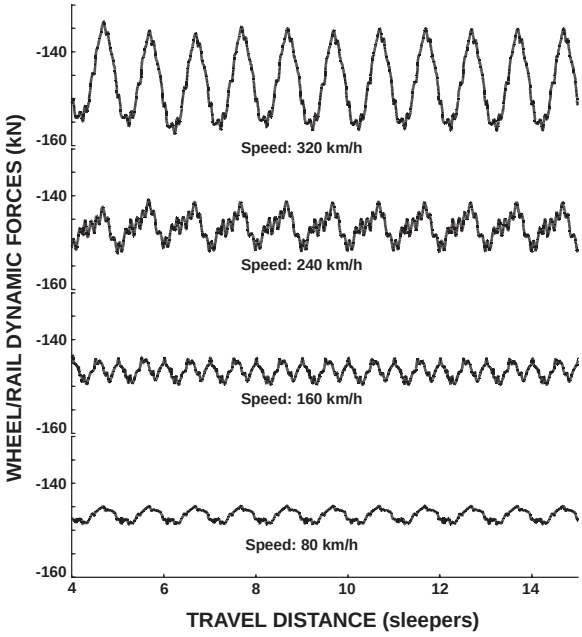

Fig. 9. Wheel/rail dynamic forces at different speeds.

vehicle–track interaction. The track parameters of the sleeper used in the present study are basically the same as those used in a previous study [12], which reported that the rigid body resonant modes of the sleeper in the track were about 73 Hz. This frequency is almost exactly the same as the sleeper passing frequency (= vehicle speed/sleeper spacing) corresponding to 160 km/h. Clearly, the rigid resonant mode of the sleeper in the track was probably excited at this speed and caused the double waves in each sleeper spacing.

4.2. Dynamic interaction for one wheel flat

It is assumed that only one wheel flat exists on the left leading wheel. The surface geometry is expressed by Eq. (9). The inputted irregularity function along with the system time history in terms of wheel/rail contact forces, displacement of sleepers, rails and wheels, forces on pads and ballast and rail acceleration are illustrated in Fig. 10. After the irregularity appears, the wheel is unloaded and the contact force quickly drops to zero; the wheel moves down and the rail rises up; the wheel loses contact with the rail for a short moment and then impacts on the rail. The impact force is larger than the static load and depends on the train speed and the size of the flat. The negative overlap of the wheel/rail displacements indicates that the wheel is separated from the rail on the wheel centreline. At the same time as the wheel impacts on the rail, the sleepers and ballast also suffer a high impact force.

Even though the defect is on the left leading wheel, the impact affects other wheels through the wheel axles and bogie. Fig. 11 exhibits the characteristics of the effects. The impact on the left leading wheel results in impact and vibration on the left trailing wheel and oscillation of the wheels on the right side.

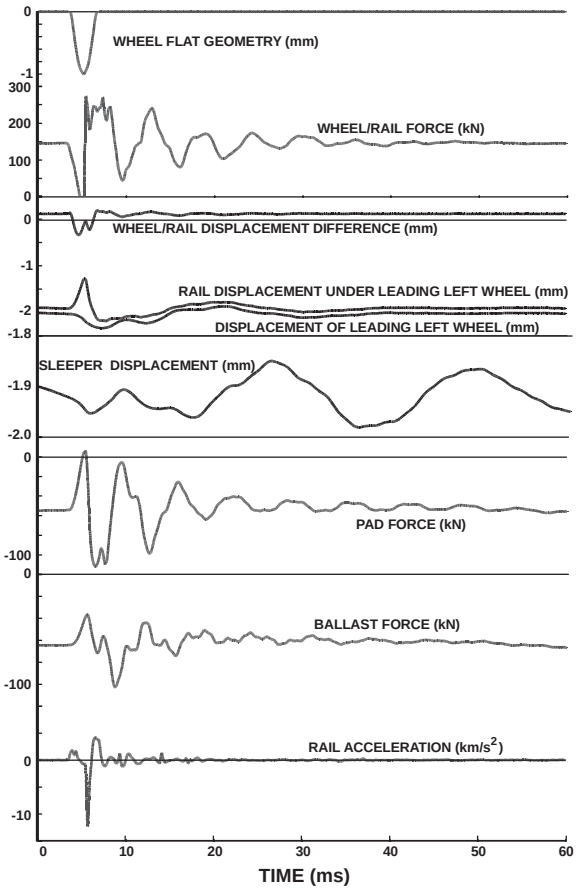

Fig. 10. Responses of forces and displacements to the wheel flat.

The characteristic of the rail acceleration is unique in comparison to other variables, as shown in Fig. 10. A very sharp acceleration peak in its time history occurs at the moment when the wheel hits the rail. Because the rail mass is much smaller than wheel mass, the rail acceleration is very sensitive to impact due to wheel/rail irregularities. This principle is used in commercial wheel impact detection devices.

5. Conclusions

A finite element time-domain model for vehicle/track dynamic interaction is proposed in this paper. The model can solve the comprehensive vehicle/track dynamic problem in the time domain. All forces, displacements, velocities and accelerations of all simulated vehicle/track components can be evaluated, and the dynamic responses to wheel/rail interaction can be determined with the computer program.

The solution of the wheel flat case reveals that the wheel/rail impact on one rail significantly affects the wheel/rail interaction on the other side of the track.

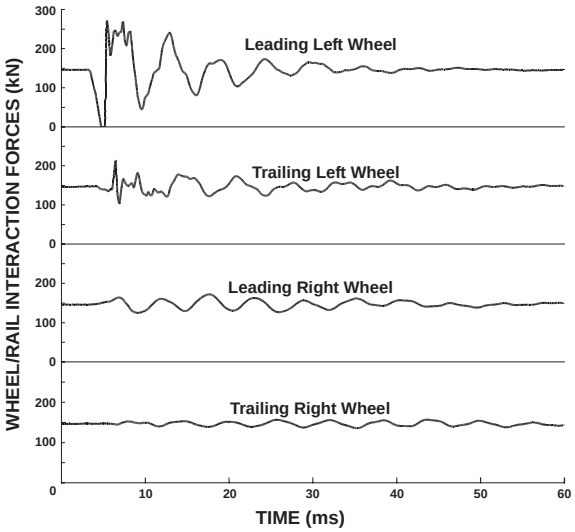

Fig. 11. Contact forces at four contact points.

Since forces and displacements of whole systems can be calculated with the computer model, the model can be used to do further vibration and noise analysis for vehicle/track components.

Appendix A. Parameters for the example cases

Track	
Rail	RE 136
Timoshenko shear coefficient of the rail	0.34
Sleeper spacing	0.6069 m
Length of the sleeper	2.36 m
Sleeper mass	180 kg
Pad stiffness (per node)	200 MN/m
Ballast stiffness (per sleeper)	40 MN/m
Pad damping (per node)	30 kN s/m
Ballast damping (per sleeper)	50 kN s/m
Vehicle	
Wheelset mass	1300 kg
Wheelset moment of inertia	1000 kg m^2
Bogie mass	500 kg
Bogie rotational moment	176 kg m^2
Car body mass (half vehicle)	56,900 kg
Wheelset axle spacing	1.778 m
Stiffness of the primary suspension	788 MN/m
Stiffness of the secondary suspension	6.11 MN/m

Damping of the primary suspension	3.5 kN s/m
Damping of the secondary suspension	15.8 kN s/m

References

[1] K.L. Knothe, S.L. Grassie, Modelling of railway track vehicle/track interaction at high frequency, *Vehicle System Dynamics* 22 (1993) 209–262.
[2] S. Timoshenko, Method of analysis of statical and dynamical stresses in rail, *Proceedings of Second International Congress for Applied Mechanics*, 1926, pp. 407–418.
[3] Y. Sato, Study on high frequency vibration in track operated with high-speed trains, *Quarterly Report of RTRI* 24 (2) (1977) 109–114.
[4] S.L. Grassie, R.W. Gregory, D. Harrison, K.L. Johnson, The dynamic response of railway track to high frequency vertical excitation, *Journal of Mechanical Engineering Science* 24 (1982) 77–90.
[5] D.J. Thompson, Wheel-rail Noise: Theoretical Modelling of the Generation of Vibrations, Ph.D. Thesis, University of Southampton 1990.
[6] Z. Cai, G.P. Raymond, Theoretical model for dynamic wheel/rail and track interaction, *Proceedings of 10th International Wheelset Congress*, 1992, pp. 127–131.
[7] J.C.O. Nielsen, Train/track Interaction, Coupling of Moving, Stationary Dynamic Systems—Theoretical and Experimental Analysis of Railway Structures Considering Wheel and Track Imperfections, Ph.D. Thesis, Chalmers University of Technology 1993.
[8] J.C.O. Nielsen, A. Igeland, Vertical dynamic interaction between train and track — influence of wheel and track imperfections, *Journal of Sound and Vibration* 187 (5) (1995) 825–839.
[9] R.G. Dong, Vertical Dynamics of Railway Vehicle-track System, Ph.D.Thesis, Concordia University 1994.
[10] R.G. Dong, S. Sankar, R.V. Dukkipati, A finite element model of railway track and its application to wheel flat problem, *Proceedings of the Institution of Mechanical Engineers 208*, Part F, 1994, pp. 61–72.
[11] W. Zhai, X. Sun, A detailed model for investigating vertical interaction between railway vehicle and track, *Vehicle System Dynamics* 23 (1994) 603–615.
[12] R.G. Dong, S. Sankar, The characteristics of impact loads due to wheel tread defects, *Rail Transportation Division, American Society of Mechanical Engineers* 8 (1994) 23–30.